J Mater Sci (2007) 42:7690–7695
DOI 10.1007/s10853-007-1684-9

Kinematical studies on rotation-based semi-auxetics

Teik-Cheng Lim

Received: 23 May 2006 / Accepted: 12 March 2007 / Published online: 3 June 2007

Abstract Auxetic materials are those which exhibit negative Poisson's ratio, i.e. these solids expand transversely when stretched longitudinally. In recent years the concept of semi-auxetics has been examined for cellular solids based on combination of re-entrant and hexagonal microstructures. In this paper we identify a type of rotating unit that gives positive Poisson's ratio so that a study can be made on rotating sub-structures that exhibit both positive and negative Poisson's ratio characteristics. A second type of rotating geometry, whose Poisson's ratio shifts from negative to positive as stretching increases, has also been identified. Based on kinematical studies we explore the relationship between the on-axis Poisson's ratios in terms of novel lattice geometry and the magnitude of deformation.

Introduction

Auxetic systems are materials and structures that exhibit negative Poisson's ratio [1, 2], and are available both as (a) naturally occurring materials such as certain cubic metals and face-centered cubic rare gas solids when stretched along [110] off-axis direction [3], α-crystobalite polymorph of crystalline silica [4] and zeolites [5, 6], as well as (b) synthesized materials such as polymeric foams [1], designed molecular network [2], metallic foams [7] and microstructural and nanostructural polymers [8–12]. Based on molecular mechanics simulation, the all-silica zeolite MFI (ZSM5-$Si_{96}O_{195}$) have been shown to possess both negative and positive on-axis Poisson's ratios [6, 13].

Semi-auxetic materials are defined as those that partially exhibit negative Poisson's ratio. They can either be materials that exhibit positive and negative Poisson's rations in different Cartesian plane, or be functionally graded structures that possess positive Poisson's ratio at one end to negative Poisson's ratio at the other end. In this paper, we analyze the concept of semi-auxetics for a typical auxetic structure that exhibits (a) plane-specific semi-auxeticity, and (b) strain-dependent auxeticity. Although the benefits of auxetic behavior are made known in most auxetic literature, it remains a fact that not all applications require or even desire auxetic behavior. Indeed, the introduction of semi-auxetic concept [14–18] aims to understand the result of combined conventional and auxetic properties for applications that require combined behavior. Unlike conventional materials and auxetic materials (Fig. 1), a plane-dependent semi-auxetic material exhibits both auxetic and conventional behavior in two of orthogonal planes, as shown in Fig. 2a and b, and conventional behavior in the third orthogonal plane, as depicted in Fig. 2c. In other words, stretching in axis-1 causes expansion along axis-2 but contraction in axis-3, whilst stretching in axis-2 leads to expansion in axis-1 but contraction in axis-3. Like conventional materials, stretching in axis-3 gives contraction in both axes 2 and 3. Not all rotating units give auxetic behavior. This differentiates the present semi-auxetic from the fully auxetic materials investigated earlier [5, 19–22].

A typical schematic for plane-dependent auxeticity is shown in Fig. 3 whereby (a) rotation about axis-3 gives auxetic behavior in plane 1–2 whilst (b) rotations about axes-1 and –2 give conventional behavior in planes 2–3 and 3–1, respectively.

T.-C. Lim (✉)
School of Science and Technology, SIM University (UniSIM), 535A Clementi Road, Singapore 599490, Republic of Singapore
e-mail: alan_tc_lim@yahoo.com

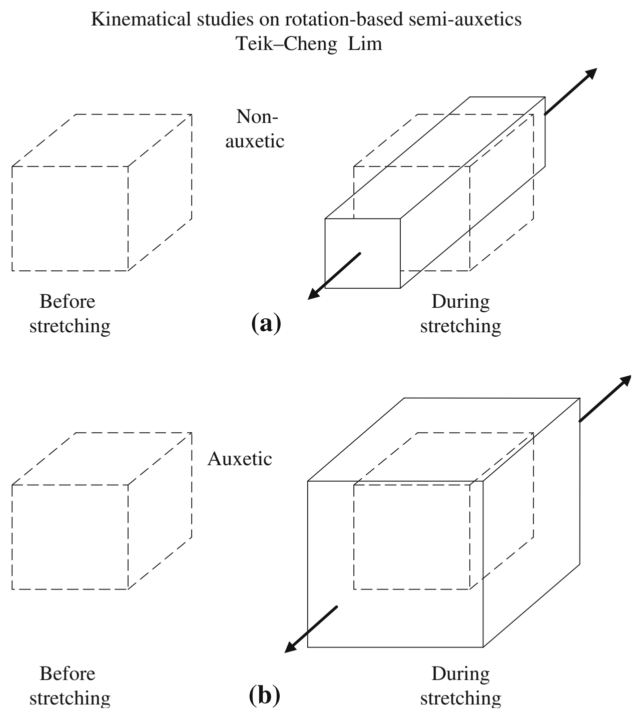

Fig. 1 Comparison between (**a**) non-auxetic (conventional) and (**b**) auxetic materials deformation when subjected to uniaxial stretching

To establish an analytical relationship between the molecular geometry and the Poisson's ratio of a generic rotation-based semi-auxetic material, we herein attempt the development of a closed-form solution of the Poisson's ratio in terms of the bond geometry and on-axis strain. As a preliminary step we introduce the concept of virtual link of length l as a function of actual bond length r, as shown in Fig. 3c. For a tetragonal structure with equal bond lengths r and bond angle Ω, $l = r\sqrt{2(1-\cos\Omega)}$ where the tetragonal angle is $\Omega = 109.5°$. The following analysis prescribes lengths l_1, l_2 and l_3 for virtual links OA, OB and OC, respectively, to cater for non-exact tetragonal structures when the central atom is bonded with more than one type of atoms—hence different bond lengths and bond angles.

Analysis

Plane-dependent auxeticity

With reference to Fig. 4a, let the rigid junction be the origin of a localized Cartesian coordinate system such that only three virtual links (OA, OB and OC) are considered for analysis. Apart from the virtual lengths, the bond angles are to be assigned. There are two approaches. The first approach assigns symbols that represent the rigid angles AOB, BOC and COA. The second approach assigns the angles made by OA, OB and OC with axes-1, –2 and –3, respectively. We select the second approach due to its ease for analysis. The projected lengths and angles on planes 1-2, 2-3 and 3-1 are shown in Fig. 4b–d, respectively, under two geometrical assumptions, i.e. (i) the angle AOB is 90° when projected on plane 1–2, and (ii) the link OC lies on axis-3. The geometrical assumptions are imposed to optimize the magnitude of the negative and positive Poisson's ratios. Apart from geometrical assumptions, we introduce kinematical assumptions. First, we assume that stretching of OA (or OB) in direction-1 (or direction-2) induces the following rotations: (a) OA rotates by φ_2 and φ_3 about axes-2 and –3, respectively, (b) OB rotates by φ_1 and φ_3 about axes-1 and –3, respectively, and OC rotates by φ_1 and φ_2 about axes-1 and –2, respectively. Second, we assume no change in bond lengths and the tetragonal angle such that the virtual link lengths of OA, OB and OC as well as the angles AOB, BOC and COA do not change. As a consequence,

$$\phi_1 : \phi_2 : \phi_3 = \theta_1 : \theta_2 : \theta_3. \tag{1}$$

The kinematical assumptions are valid due to the highly compliant rotating hinge by comparison with the almost rigid tetrahedral structure. The projected lengths of OA and OB on axes-1 and –2 are

$$(L_i)_0 = l_i \cos\theta_j \cos\theta_3; \quad i,j = 1,2 \tag{2}$$

before deformation and

$$L_i = l_i \cos(\theta_j - \phi_j)\cos(\theta_3 - \phi_3); \quad i,j = 1,2 \tag{3}$$

during deformation, whilst the projected lengths of OC on axis-3 are

$$(L_3)_0 = l_3 \tag{4}$$

before deformation and

$$L_3 = l_3 \cos\phi_1 \cos\phi_2 \tag{5}$$

after deformation. As such, the normal strains in directions-1 and –2 are

$$\begin{aligned}\varepsilon_i &= \frac{L_i - (L_i)_0}{(L_i)_0}\\ &= \left(\cos\phi_j + \tan\theta_j \sin\phi_j\right)(\cos\phi_3 + \tan\theta_3 \sin\phi_3) - 1\end{aligned} \tag{6}$$

for $i,j = 1,2$, whilst the normal strain in direction-3 is

$$\varepsilon_3 = \frac{L_3 - (L_3)_0}{(L_3)_0} = \cos\phi_1 \cos\phi_2 - 1. \tag{7}$$

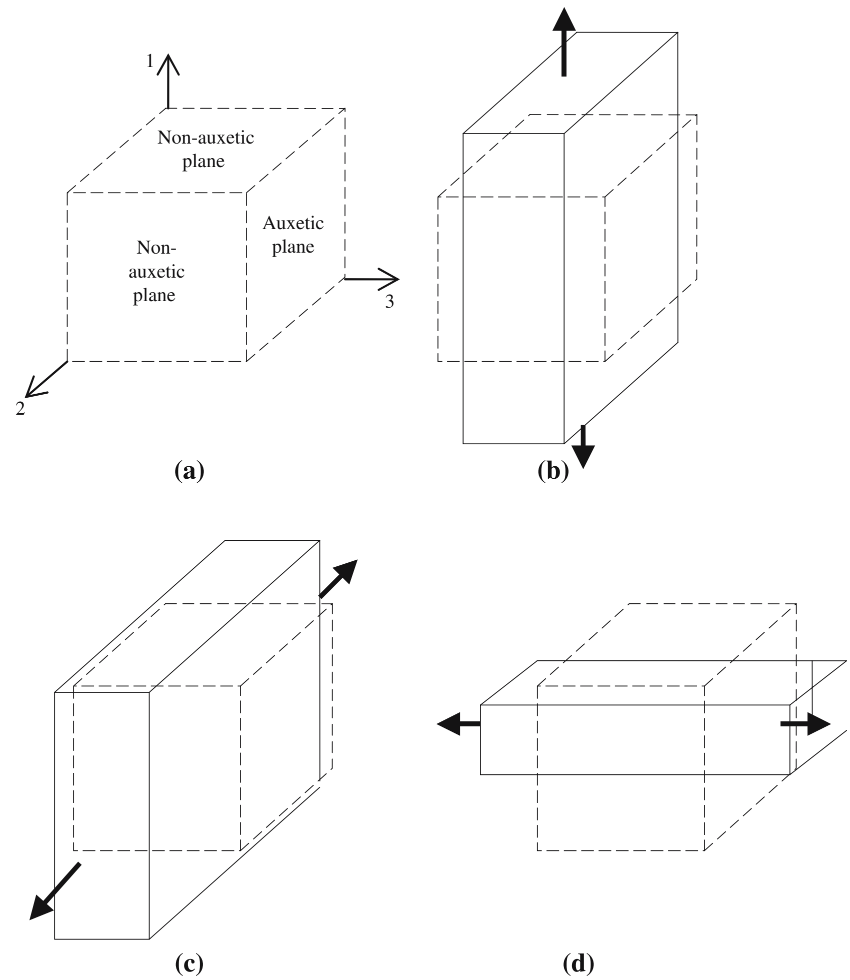

Fig. 2 Schematic description of a plane-dependent semi-auxetic material: (**a**) a sample material exhibiting auxetic behavior in plane 1–2 only, (**b**) stretching in axis-1 direction, (**c**) stretching in axis-2 direction, and (**d**) stretching in axis-3 direction

Hence the Poisson's ratios are obtained as

$$v_{ij} = \frac{1}{v_{ji}} = -\frac{\varepsilon_j}{\varepsilon_i} = \frac{(\cos\phi_i + \tan\theta_i \sin\phi_i)(\cos\phi_3 + \tan\theta_3 \sin\phi_3) - 1}{1 - \left(\cos\phi_j + \tan\theta_j \sin\phi_j\right)(\cos\phi_3 + \tan\theta_3 \sin\phi_3)} \tag{8}$$

and

$$v_{3i} = \frac{1}{v_{i3}} = -\frac{\varepsilon_i}{\varepsilon_3} = \frac{\left(\cos\phi_j + \tan\theta_j \sin\phi_j\right)(\cos\phi_3 + \tan\theta_3 \sin\phi_3) - 1}{1 - \cos\phi_i \cos\phi_j} \quad \text{for } i,j = 1,2. \tag{9}$$

Strain-dependent auxeticity

Recall that the first geometrical assumption sets the angle AOB as 90° when projected on lane 1–2. In the second part of our analysis, we relax this imposition to investigate the influence of angle AOB on the in-plane Poisson's ratio. Suppose OA and OB now lies on plane 1–2 subtended by angles α and β with respect to axes-1 and –2, respectively, as shown in Fig. 5. The following analysis takes on all other assumptions and methodology stated in Sect. 2.1. Under the influence of a force F acting on point A in the direction of axis-1, AOB rotates by an angle φ such that

$$\begin{Bmatrix} \varepsilon_A \\ \varepsilon_B \end{Bmatrix} = \begin{bmatrix} 1 & \tan\alpha \\ 1 & \tan\beta \end{bmatrix} \begin{Bmatrix} \cos\phi \\ \sin\phi \end{Bmatrix} - \begin{Bmatrix} 1 \\ 1 \end{Bmatrix}, \tag{10}$$

thereby giving the Poisson's ratio in plane 1–2 as

$$v_{AB} = -\frac{\varepsilon_B}{\varepsilon_A} = \frac{(\cos\phi + \tan\beta \sin\phi) - 1}{1 - (\cos\phi + \tan\alpha \sin\phi)}. \tag{11}$$

Since the application of force F aligns OA to axis-1 by rotating OAB by an angle φ (see Fig. 5), then the extent of auxeticity is dependent on the angle β with respect to α. We identify three cases: (i) $0 < \alpha < \beta$, (ii) $\beta < \alpha < 2\beta$, and (iii) $2\beta < \alpha < (\pi/4)$.

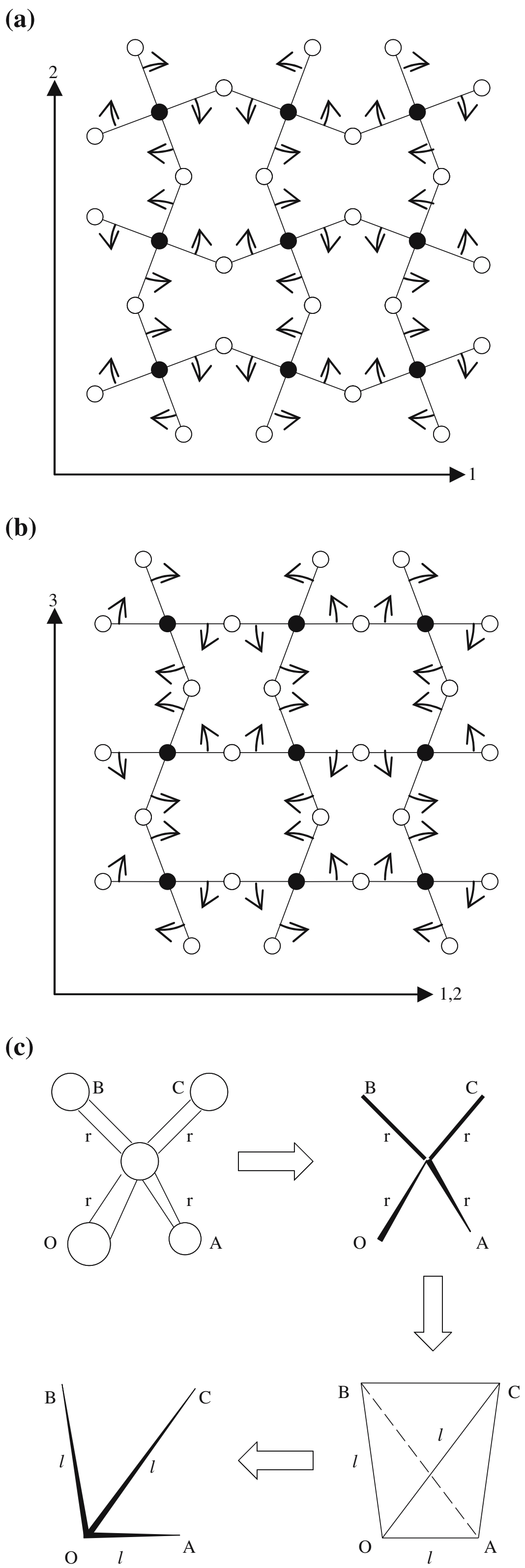

Fig. 3 Example of a zeolite-like structure that exhibits auxetic behavior in (**a**) plane 1–2, (**b**) conventional behavior in planes 1–3 and 2–3, and (**c**) concept of virtual links for analysis. Only plane 1–2 is similar to earlier auxetic works [5, 19–22] while planes 1–3 and 2–3 are representative of non-auxetic behavior

In the first case where $\alpha < \beta$, OB retains in its quadrant even after a complete rotation of $\varphi = \alpha$ for placing OA on axis-1. This ensures complete auxeticity throughout the entire stretching. For the second case where $\alpha \in [\beta, 2\beta]$, a partial rotation of $\varphi = \beta$ aligns OB on axis-2 while OA remains in its original quadrant. Subsequent rotation pushes OB into its neighboring quadrant, thereby decreasing the magnitude of the transverse strain. The overall Poisson's ratio remains negative, although to a lower magnitude. In the third case whereby $\alpha > 2\beta$, a partial rotation of $\varphi = 2\beta$ pushes OB to the other side of axis-2 in such a manner that the new location forms a mirror image of its original position about the same axis. At this juncture, the Poisson's ratio is zero. Subsequent rotation causes overall negative transverse strain, or positive Poisson's ratio, thereby ending the auxeticity.

Results and discussion

For illustration purposes we consider a special case whereby $\theta_1 = \theta_2 = \theta_3 \equiv \theta$. As a result of the second kinematical assumption described in Eq. 1, we have $\phi_1 = \phi_2 = \phi_3 \equiv \phi$. Therefore Eqs. 6–9 reduce to

$$\varepsilon_i = (\cos\phi + \tan\theta\sin\phi)^2 \tag{12}$$

$$\varepsilon_3 = \cos^2\phi - 1 \tag{13}$$

$$v_{ij} = v_{ji} = -1 \tag{14}$$

$$v_{3i} = \frac{1}{v_{i3}} = \frac{(\cos\phi + \tan\theta\sin\phi)^2 - 1}{1 - \cos^2\phi} \tag{15}$$

for i,j = 1,2. Fig. 6a shows the variation of the Poisson's ratios on three orthogonal axes with reference to in-plane strain ε_i (i = 1,2) for $\theta = 20°$. Whilst it is obvious that $v_{12} = v_{21} = -1$, we note positive and negative Poisson's ratio are exhibited for tensile and compressive loading respectively in the other two orthogonal planes—hence the Poisson's ratio being plane-dependent and loading direction-dependent. Quantitatively, $|v_{i3}| < |v_{ij}| < |v_{3i}|$. Figure 6b demonstrates the influence of θ and positive in-plane strain on v_{i3}; (i = 1,2), bearing in mind the reversal of Poisson's ratio sign when the strain is negative. It can be seen that (i) the Poisson's ratio increases in an exponential-like manner with strain, and that (ii) the Poisson's ratio is lower when the offset angle θ is larger.

Figure 7 shows the change in the in-plane Poisson's ratio with ε_A for various combinations of α and β with $\alpha + \beta = 30°$. For illustration purposes, we set the combination as a variation of α and β at increasing and decreasing intervals of 2.5° respectively, i.e. (α,β) = (12.5°,17.5°), (15.0°,15.0°), (17.5°,12.5°), (20.0°,10.0°) and (22.5°,7.5°).

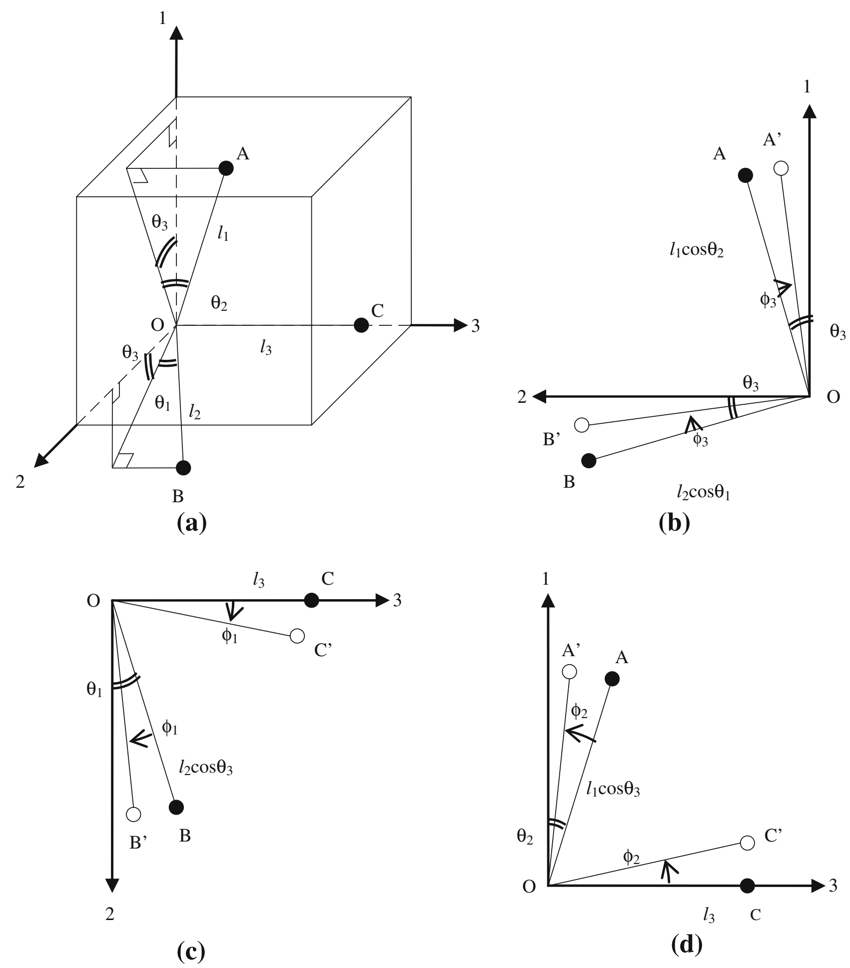

Fig. 4 Schematics for plane-dependent auxeticity: (**a**) isometric view of bonds virtual links OA, OB and OC of lengths l_1, l_2 and l_3 respectively, with the undeformed state bolded, (**b**) the projected lengths of OA and OB on plane 1–2 are $l_i \cos\theta_j$; ($i,j = 1,2$), whilst (**b**), (**c**) the projected lengths of OA and OB are $l_i \cos\theta_3$; ($i = 1,2$) on the other two orthogonal planes

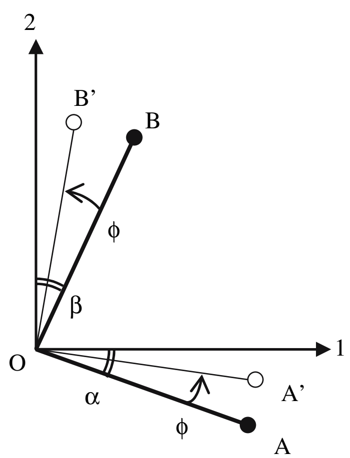

Fig. 5 Schematic for analysis of strain-dependent auxeticity

The first, third and fifth combinations simulate examples for regions $0 < \alpha < \beta$, $\beta < \alpha < 2\beta$ and $2\beta < \alpha < 90°$ respectively whilst the second and fourth combinations illustrate the boundary conditions of $\alpha = \beta$ and $\alpha = 2\beta$ respectively. Plotted result reveals that (i) the magnitude of Poisson's ratio in this auxetic system increases with the reduction of (α/β) ratio, and (ii) the possibility of negative Poisson's ratio to drop to zero and followed by entrance into the positive region when $\alpha \geq 2\beta$.

Conclusions

This paper first shows that not all rotating units exhibit auxetic behavior, and that rotating units that exhibit auxetic and non-auxetic characteristics can be combined to give plane-strain semi-auxetic materials. Second, it has been shown that, based on specific geometrical properties, some rotating structures that exhibit auxetic properties during the initial stage of deformation tends to change in their behavior towards non-auxetic properties when the deformation exceed certain magnitude. These two new rotation-based geometrical structures, which give plane-dependent and strain-dependent semi-auxetic behavior, have been identified. A kinematical study has been performed on these two structures to observe the quantitative extent of the Poisson's ratio. It has been shown that for

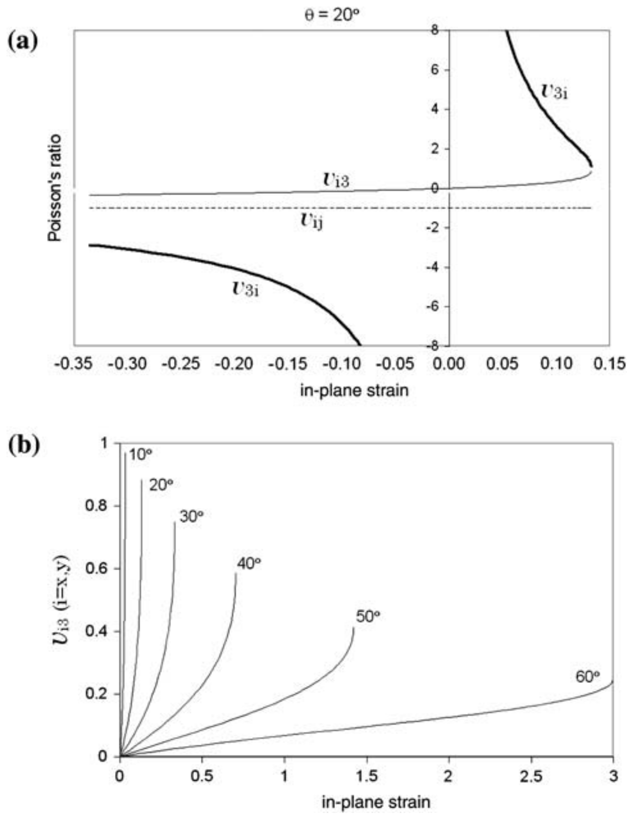

Fig. 6 (**a**) The change in Poisson's ratio in three orthogonal planes with respect to in-plane strain at $\theta = 20°$, and (**b**) the change in out-of-plane Poisson's ratio with respect to in-plane strain for various θ

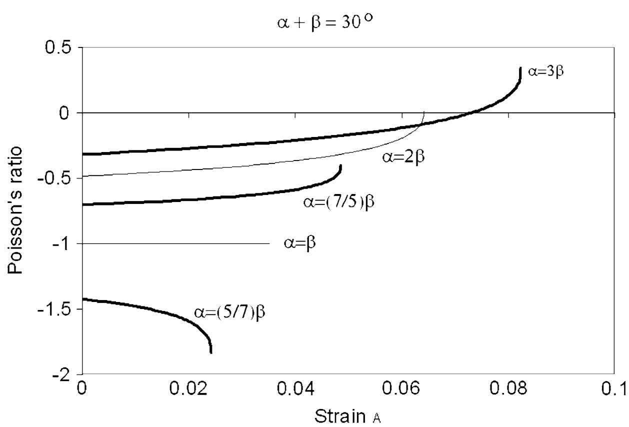

Fig. 7 The change in the in-plane Poisson's ratio with respect to strain in loading direction for various combinations of α and β whereby $\alpha + \beta = 30°$

plane-dependent semi-auxetic materials, all three orthogonal planes exhibit auxetic behavior during compressive loading but two of these planes exhibit positive Poisson's ratio during tensile loading. For the case of strain dependent semi-auxetic materials, it has been shown that both the undeformed geometry and extent of strain strongly influence the magnitude of the Poisson's ratio. In contrast to the closed-form solution demonstrated in this paper, molecular modeling approach is suggested for future work on studying molecular semi-auxetics. Having demonstrated the possibility of rotation-based semi-auxetics by analytical approach, more refined results can be expected when the change in bond length and bond angle are taken into account.

References

1. Lakes R (1987) Science 235:1038
2. Evans KE, Nkansah MA, Hutchinson IJ, Rogers SC (1991) Nature 353:124
3. Baughman RH, Shacklette JM, Zhakhidov AA, Stafstrom S (1998) Nature 392:362
4. Yeganeh-Haeri Y, Weidner DJ, Parise JB (1992) Science 257:650
5. Grima JN, Evans KE (2000) J Mater Sci Lett 19:1563
6. Grima JN, Jackson R, Alderson A, Evans KE (2000) Adv Mater 12:1912
7. Choi JB, Lakes R (1995) Int J Mech Sci 37:51
8. Alderson KL, Evans KE (1993) J Mater Sci 28:4092
9. Alderson A, Evans KE (1997) J Mater Sci 32:2797
10. Lu XH, He CB, Terrell CD, Griffin AC (2002) Macromol Chem Phys 203:85
11. He CB, Liu PW, Griffin AC, Smith CW, Evans KE (2005) Macromol Chem Phys 206:233
12. Lu XH, He CB, Liu PW, Griffin AC (2005) J Polym Sci Part A: Polym Chem 43:3394
13. Alderson A, Davies PJ, Evans KE, Alderson KL, Grima JN (2005) Mol Simul 31:889
14. Lim TC (2002) J Mater Sci Lett 21:1595
15. Lim TC (2002) J Mater Sci Lett 21:1899
16. Lim TC (2003) J Mater Sci Lett 22:1783
17. Lim TC (2004) J Mater Sci 39:4965
18. Lim TC (2005) J Mater Sci 40:3275
19. Grima JN (2005) In: Proceedings of the 2nd workshop on auxetics and related systems, Poznan
20. Grima JN (2000) PhD Thesis, Exeter University
21. Vasiliev AA, Dmitriev SV, Ishibashi Y, Shigenari T (2002) Phys Rev B 65:094101
22. Ishibashi Y, Iwata M (2000) J Phys Soc Jpn 69:2702